Combining transient and continuous identification techniques to investigate human reflexes

MSc Thesis

Ivo Ulrich

September 13, 2012

Student number:	4117859
Department number:	1342
MSc-Thesis Advisors:	Dr. ir. Winfred Mugge
	Dr. ir. Alfred C. Schouten
	Prof. Dr. Frans C.T. van der Helm

TU Delft Delft University of Technology

Neuromuscular Control Laboratory
Department of Biomedical Engineering
Faculty of 3mE

Contents

Abstract

In many everyday activities such as steering a bicycle, unpredictable mechanical disturbances trigger quick involuntary and situation-specific reactions via neural loops generally referred to as reflexes. Research investigating reflexes via transient perturbations elicit muscle activations typically observed as two distinct responses in an electromyography with the short-latency response M1 viewed as stereotyped and task-independent and the long-latency response M2 seen as task-dependent. In contrast, task-dependency of short-latency pathways (specifically velocity and force feedback) was demonstrated by studies using continuous perturbations and system identification techniques to separate reflex from voluntary contributions. This study addressed the opposing experimental findings by isolating reflex contributions in the human wrist joint using both the transient and the continuous approach simultaneously in conditions where reflex modulation is expected. Subjects (n = 11) held a manipulator handle which applied mechanical perturbations and imposed a virtual mechanical environment to the wrist. Increasing damping of the environment and reduced continuous perturbation bandwidth in a "maintain position" task (PT) decreased the subject's mechanical joint admittance, increased excitatory velocity and force feedback obtained from a neuromuscular model, increased M2 but did not affect M1. Instructing subjects to "maintain force" increased the joint admittance, decreased M2 and counterproductive to the task increased M1 with respect to the PT. Results from this study indicate that the continuous approach does not condition M1 and that the reflexive feedback from short-latency pathways obtained via the presented neuromuscular model does not directly map to the M1 elicited by transient perturbations.

1 Introduction

In everyday activities humans cope with mechanical disturbances from the environment. For example when holding an umbrella against brief gusts of wind or when drinking a cup of tea on the back seat of a car. Humans react quickly to unpredictable external disturbances that interfere with the current objective and adapt these reactions to the specific situation. Sensory units, which provide information about muscle stretch or force, are embedded in neural loops that trigger quick involuntary reactions generally referred to as reflexes. Past and current research is interested in characterizing how corrections initiated from reflexive feedback are related to unexpected mechanical disturbances to obtain a full understanding of the function of reflex pathways in the control of movement. Manipulators apply controlled mechanical perturbations to joints and reflex activity is quantified based on measured signals such as position, force or muscle activation. Studies that evoke reflexes via mechanical disturbances can be divided into two groups, the one using: brief, transient perturbations and the other using continuous perturbations.

When a brief stretch such as a ramp-and-hold displacement is applied to an active muscle a muscle activation is evoked. The muscle activation can typically be observed in an electromyography (EMG) as two distinct responses, which Lee and Tatton (1975) named M1 for the initial short- and M2 for the later long-latency response. Medication (Meskers et al. 2010), local anesthesia (Grey et al. 2001) and other tools have been used together with transient perturbations to isolate certain reflexive pathways and to link the observed M1 and M2 to their physiological origin. M1 is agreed to originate from stretch receptors within the muscles called muscle spindles (MS), specifically from Ia afferents providing information on the muscle stretch velocity which have a direct excitatory connection via the spinal cord back to the muscle (Kandel et al. 2000). The origin of M2 is unknown, contributions from slower sensory feedback like MS length feedback (II afferents) and cutaneous afferents or trans-cortical pathways have been suggested (Corden & Lippold 2000, Grey et al. 2001, Meskers et al. 2010). Studies applying transients used different motion control tasks instructing subjects to minimize displacements (position task) or force deviations (force task) to investigate adaptation of M1 and M2. The task dependence of M1 is uncertain and disagreed upon while the modulation of M2 is not questioned (Shemmell et al. 2010). The short nature of the transients may not allow proper conditioning of a subject's state of the reflex pathways. Another limitation is that to be able to draw conclusions from observed changes in the transient response one has to precisely control the afferent input i.e. position, velocity information which is most accurately done by position perturbations, dictating the joint position. However, studies using transients benefit from the straightforward reflex assessment: isolating reflex activation by processing the EMG after perturbation onset.

The second approach uses continuous perturbations which consistently evoke reflexive activity by continuous afferent stimulation. The EMG does not show a clear identifiable M1 and M2 but instead reflex activation is blended together with voluntary activation. System identification and modeling techniques are needed and used to quantify reflexes (Kearney et al. 1997, Van Der Helm et al. 2002). Reflex gains are determined via neuromuscular models based on their contributions to the overall

mechanical behavior on the joint level. Such models are based on assumptions as for example what physiological components to include and if the observed behavior is linear or non-linear. The reflex gains represent the amplification factor of a specific sensory input to a reflexive muscle force and include a variety of physiological processes which makes interpretation of the results necessary to map findings to physiology. Schouten (2004) showed that during a position task joint admittance, the relation between an input force and the resulting joint motion, decreased when stability provided by an external environment is increased or when the bandwidth of the applied perturbation is reduced. The observed modulation was attributed to an increase in reflex activity, specifically in the velocity feedback (representing MS feedback). Mugge (2011) found a significant role for force feedback, Golgi tendon organs (GTO) situated in the muscle tendon providing information through Ib afferents, with inhibitory and excitatory behavior in a context-dependent manner in a position and force task experiment. Schouten (2004) and Mugge (2011) mainly ascribed the observed reflex adaptation to fast short-latency pathways, velocity and force feedback. Studies using continuous perturbations provide subjects with continuous afferent information which results in a more defined way of conditioning the subject's state of the reflex pathways. Furthermore, the choice of perturbation type i.e. position or force perturbation is not prescribed by the method.

1.1 Problem Statement and Goal

Studies using transient perturbations mostly demonstrated a task-independent M1 and have consolidated the view of M1 as being a stereotyped velocity-dependent reflex (Doemges & Rack 1992, Kurtzer et al. 2008, 2010, Lewis et al. 2006, Pruszynski et al. 2008). In contrast, a group of studies using continuous perturbations showed the importance of short-latency pathways in contributing to a task-dependent mechanical behavior (De Vlugt et al. 2002, Mugge 2011, Schouten 2004). The inconsistencies in the experimental findings still leave the question whether or not the human is able to adjust the short-latency response unanswered. Only a better understanding of the methods' inherent differences and their specific influence on the experimental findings can eliminate the doubts that persist for many years and help to improve the design of experiments in the future.

The goal of this study is to quantify proprioceptive reflexes with both the transient and the continuous approach simultaneously and to determine how these approaches influence the experimental findings themselves.

1.2 Hypotheses

1. In a position task, an increase in external damping or a decrease in perturbation bandwidth will
    a) decrease the joint admittance and increase the excitatory reflexive feedback, primarily velocity feedback (Schouten 2004).
    b) result in an increase in M1 amplitude.
2. In respect to a position task, a force task results in
    a) an increased joint admittance and decreased excitatory (position and velocity feedback) but increased inhibitory reflexive feedback (force feedback) (Mugge 2011).
    b) smaller M1 and M2 amplitudes.

2 Method

2.1 Subjects

11 healthy right-handed subjects (mean age of 25.9 (standard deviation 1.87) years, 4 women) participated in the experiment. The experiment was carried out on the right wrist. The subjects had no prior history of neurological disorders with extremity involvement, other diseases or surgery to the right arm/wrist. All subjects provided written informed consent prior to the experiment. The study was approved by the Delft University of Technology Ethics Committee.

2.2 Experimental Setup

Torque and position perturbations were applied at the wrist using a wrist manipulator (see Figure 1, (Schouten et al. 2006)). Subjects sat in a chair, holding the handle with the right hand, while the forearm was restrained in an arm support to align the manipulators axis of rotation with the wrists' flexion-extension axis. Muscle activation signals (EMG) of one wrist flexor (flexor carpi radialis, FCR) and one wrist extensor (extensor carpi radialis, ECR) were recorded via surface electrodes placed on the forearm. A monitor in front of the subject provided task-related visual feedback to prevent drift from the reference.

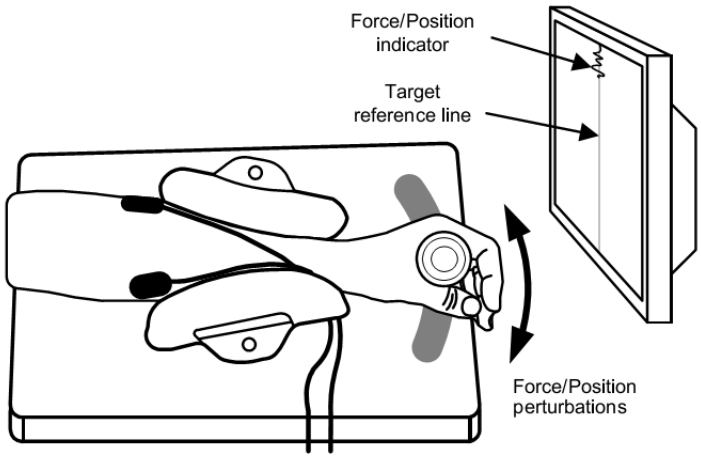

Figure 1: Experimental setup. The subject is seated in upright position with a fixated forearm to align the manipulators axis of rotation with the wrists' flexion-extension axis. The actuated handle applied torque or position perturbations in the wrist's flexion/extension direction. A monitor in front of the subject provided task-related visual feedback. Two electrodes were placed on the forearm to record activation signals of one wrist flexor (flexor carpi radialis) and one wrist extensor (extensor carpi radialis).

2.3 Experimental Protocol

2.3.1 MVC

Subjects were asked to push and pull as hard as they could in the flexion and extension direction (called maximum voluntary contraction, MVC), while the handle was fixed in the wrists' neutral position, the position when the subject was relaxed. The torques and EMG signals were recorded during two repetitions for each direction. The MVC measurement was done at the beginning and end of the experiment to verify that subjects obtained enough rest during the experiment and were not fatigued.

2.3.2 Ramp Sequence

Subjects performed a task where a series of ramp-and-hold displacements was applied, similar to the procedure described in Schuurmans et al. (2009) which used a paradigm typical for studies applying only transient perturbations. The manipulator was in position control to apply ramp-and-hold displacements in extension direction with an amplitude of 0.1 rad and a velocity of 1.5 rad/s . The amplitude and velocity was based on Schuurmans et al. (2009) who investigated the stretch duration effect of M2 and reported both an M1 and an M2 using these perturbations. With the wrist in the neutral position the subject was instructed to maintain a constant flexion torque. The task instruction was to "do not intervene" with the perturbations. The applied torque at the handle was low-pass filtered at 1 Hz and displayed on the screen together with the flexion target torque ($10, 25, 40\,\%$ of the subject's maximum voluntary torque produced in flexion direction) to provide feedback. Each target torque condition ($M10R$, $M25R$, $M40R$) was composed of 2 trials with 5 ramp-and-hold displacements each. The intervals between perturbations were of randomized duration between 2.5 and 4.5 s, giving trial lengths of $\sim 20 - 25$ s.

2.3.3 Main Experiment

Subjects subsequently performed two motor control tasks while facing continuous and transient perturbations: "maintain position, minimize position deviations" (position task, PT) or "maintain force, minimize force deviations" (force task, FT). To account for the different levels of flexor activation expected during PT and FT which knowingly influence the transient response (Pruszynski et al. 2009, Toft et al. 1989) bias forces were applied in extension direction in the PT while different flexion target force levels were required in the FT (both measures will be referred to as "bias force"). Each task was preceded by a 5 minute break to prevent fatigue and a 15 minute training session to familiarize the subjects with the task. A total of 8 different conditions was applied (5 conditions PT and 3 FT, summarized in Table 2.1). Conditions were presented in randomized order within each task to avoid anticipation by the subject and were repeated 5 times, giving a total of 40 trials of ~ 45 s. In between trials the subjects could rest at their own discretion to prevent fatigue. Each trial in the main experiment consisted of two segments; each composed of a continuous force perturbation of ~ 17 s and a randomly timed transient position perturbation in extension direction of 400 ms (see Figure 2). The transient perturbation was of the same amplitude and velocity as in the ramp sequence task. Each ramp-and-hold had a 100 ms silent period of zero velocity and zero displacement before and after the ramp-and-hold. The transient perturbation was randomly timed within a 4 s window during which the continuous perturbation was still on. In case of continuous force perturbations the manipulator had to be switched from force to position control before applying the transient perturbation. To create a smooth transition from force to position perturbations the manipulator was only switched into position mode when close to the wrist's neutral position ($< |0.003\ rad|$) and when velocity was low ($< |0.0873\ rad/s|$, further details are given in the Appendix B). These values were derived from pilot experiments and ensured that no steplike perturbation was introduced by changing the manipulator settings. To prevent subjects from associating the second transient perturbation with the trial end and thereby circumvent anticipation to influence the last transient response an additional continuous perturbation of random length ($2-4$ s) was placed at the end of every trial.

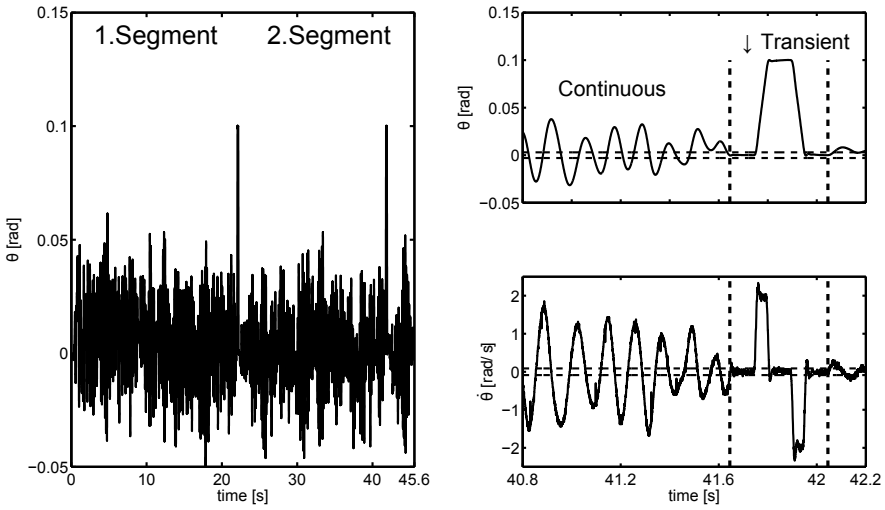

Figure 2: Left: Main experiment trial. Composed of two segments each built of one continuous ($\sim$ 17 s) and one transient (400 ms, apparent as peak of 0.1 rad) perturbation. Both segments contained a different multisine realization. Additional continuous perturbation of random length ($2 - 4$ s) at the trial end prevented anticipation of trial termination. Right: Same trial as left, zoomed into the transition from continuous to transient perturbation. Transient perturbations were only applied when wrist movements were small ($\theta < |0.003|$ rad and $\dot{\theta} < |0.0873|$ rad/s, marked with two dashed horizontal lines in the respective figure).

Subjects performed the two motor control tasks, in the following order:

1. Position task (PT), i.e., maintain position, minimize position deviations

   Continuous force perturbations (FP) were applied at the wrist while the manipulator behaved like a rotational inertia-spring-damper system. The simulated external damping (b_e) was altered between 0 and 2 Nms/rad while the external inertia ($I_e = 1.6$ gm^2) and stiffness were constant ($k_e = 0.1$ Nm/rad) during all conditions. Three levels of bias force in extension direction (0, 10, 25 % $T_{MVC,flex}$) were applied on top of the force perturbations. The angle of the handle was plotted on the monitor against a vertical reference line indicating the target angle (0° wrist flexion).

2. Force task (FT), i.e., maintain force, minimize force deviations

   The manipulator settings were changed so that it behaved as "infinitely" stiff, thus applying continuous position perturbations (PP). This was done to prevent a possible drift of the wrist angle and ensure that the transient perturbations were always applied from 0° wrist flexion. Visual feedback of the torque exerted on the handle was plotted against a vertical reference line indicating the target torque (0, 10, 25 % $T_{MVC,flex}$ in flexion direction).

The continuous force and position perturbations were designed in the frequency domain as so called multisine signals with a constant signal power and optimized crest factor (compactness of the signal) (Pintelon & Schoukens 2001, Schouten et al. 2008a). Inverse Fourier transform yielded unpredictable time signals with a duration of $\sim$ 17 s.

Two types of multisine perturbations with different frequency content were applied:

1. Wide bandwidth (WB): a perturbation signal with equal power at linearly-spaced frequencies between $0.5 - 20\ Hz$.

2. Reduced power (RP): a perturbation signal with full power between $0.13 - 1.2\ Hz$ and 0.6 % of the full power from $1.2 - 40\ Hz$, which enabled system identification and parameter fits at higher frequencies, while still evoking behavior adapted to low-frequency perturbations (Mugge & Abbink 2007).

The spectra of the continuous perturbation signals applied in both tasks are shown in Figure 3. As position perturbations were applied during the FT, the manipulator imposed the position on the subject's wrist irrespective of the subject's generated hand force. Since the subject's admittance no longer influences the handle position applying the RP force perturbation used in the PT as position perturbation in the FT would result in a high-frequency position spectrum. The RP position perturbation was therefore filtered by a wrist joint admittance estimated in a previous FT experiment (model parameters used are given in the Appendix Table A.1).

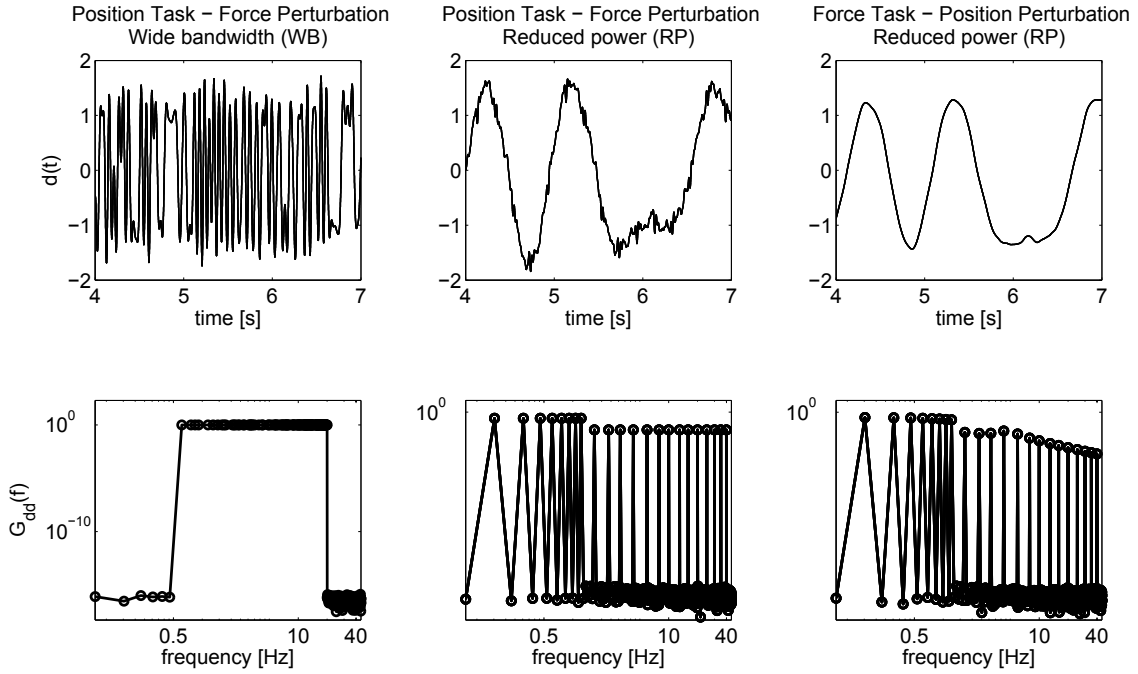

Figure 3: Perturbations signals. Upper plots: 3 s fragment of the signal in time; lower plots: power spectral density of the signals. Signals are scaled to have a standard deviation of 1°.

The continuous perturbation magnitudes were scaled for each subject and condition to obtain equal standard deviations (SD) of 1° wrist displacement to facilitate linear analysis. The scaling of the force perturbation amplitudes was determined during training trials while the amplitudes of the position perturbations were scaled off-line to SD 1°. Each segment within a trial consisted of a different multisine realization.

Table 2.1: Experimental conditions of the main experiment. (WB - wide bandwidth, RP - reduced power, PP - position perturbation, FP - force perturbation)

Perturbation Type	**Condition Name**	**Damping** $[Nms/rad]$	**Bias Force** $[\% T_{MVC,flex}]$
Position Task			
WB - FP	B00P	0	0
	B02P	2	0
RP - FP	M00P	0	0
	M10P	0	10
	M25P	0	25
Force Task			
RP - PP	M00F		0
	M10F		10
	M25F		25

2.4 Data Recording and Processing

The manipulator angle $\theta(t)$ and angular velocity $\dot{\theta}\ (t)$, the torque exerted on the handle by the subject $T(t)$, the external torque perturbation applied by the manipulator $d(t)$, and the surface EMG of the flexor carpi radialis (FCR, EMG_{flex}) and extensor carpi radialis (ECR, EMG_{ext}) were recorded with a sample frequency of 2500 Hz and a resolution of 16 bits. The EMG signals were recorded with differential surface electrodes and prior to sampling amplified by a Bagnoli desktop amplifier with a band-pass filter of $20 - 450$ Hz. The recorded EMG signals were further processed by removing power at $50, 100, 150$ Hz via a discrete Fourier Transform (DFT) line noise filter to reduce electric interference from the power grid. Finally, the EMG was rectified and low-pass filtered at 80 Hz (recursive third-order Butterworth).

2.4.1 MVC

The maximum values of the torque ($T_{MVC,flex}$, $T_{MVC,ext}$) and rectified EMG signals ($EMG_{MVC,flex}$, $EMG_{MVC,ext}$) were calculated for FCR and ECR from the MVC trials. The torque signal was filtered with a moving average filter with a 100 ms time window to determine the maximum torque of two repetitions. The corresponding EMG MVC level was then determined by taking the mean rectified EMG signal of 1 s centered around the time instant of maximum torque.

2.4.2 Transient Analysis

The EMG recordings were divided into parts starting 200 ms prior to and ending 100 ms after the onset of a ramp-and-hold perturbation. The parts were averaged over a total of 10 repetitions (ramp sequence: 2 trials $\times$ 5 ramps; main experiment: 5 trials $\times$ 2 segments). The mean background EMG of FCR $EMG_{BG,flex}$ and ECR $EMG_{BG,ext}$ were determined by the mean EMG 200 ms prior to ramp onset. M1 and M2 responses were then determined from the FCR EMG in $\%MVC$ ($M1_{MVC}$, $M2_{MVC}$) and the EMG normalized to $EMG_{BG,flex}$ ($M1_{BG}$, $M2_{BG}$). Normalized EMG values smaller than one indicate depression with respect to the background EMG and values greater than one indicate excitation. The magnitude of M1 was defined as the mean value of EMG in the time window between 20 and 50 ms after stretch onset and the magnitude of M2 as the mean value between 55 ms and 100 ms (Schuurmans et al. 2009).

2.4.3 Continuous Analysis

Non-parametric System Identification

For each condition of the main experiment the recorded signals ($\theta(t)$, $T(t)$, $d(t)$) were transformed to the frequency domain by fast Fourier transform (FFT). The first 4 s ($\sim 2^{13}$ samples) were omitted to eliminate the effects of initial adaptation after the perturbation onset, leaving 13.1072 s (2^{15} samples) for analysis. Non-parametric estimations of the human wrist admittances (FRF) were calculated using cross-spectral densities.

As force perturbations were applied during the PT, interaction between the subject and manipulator existed (the manipulator position depended on both the subject dynamics and the external environment imposed by the manipulator). Therefore a closed loop identification algorithm was required to estimate the subject's wrist dynamics. The relationship between the hand reaction force (input) and the hand position (output), i.e. the wrist admittance, was estimated by:

$$\hat{H}_{T\theta}(f) = \frac{\hat{G}_{d\theta}(f)}{\hat{G}_{dT}(f)}$$

Where $\hat{H}$ denotes the estimated FRF. The term $\hat{G}_{d\theta}$ is the cross-spectral density of $d\,(t)$ and $\theta\,(t)$, whereas $\hat{G}_{dT}$ is the cross-spectral density of $d\,(t)$ and $T\,(t)$.

As position perturbations were applied during the FT, the hand force generated by the subject no longer influenced the manipulator position. An open-loop identification algorithm was therefore used to estimate the subject's wrist dynamics:

$$\hat{H}_{T\theta}(f) = \frac{\hat{G}_{\theta\theta}(f)}{\hat{G}_{\theta T}(f)}$$

$\hat{G}_{\theta T}$ is the cross-spectral density of $\theta\,(t)$ and $T\,(t)$, while $\hat{G}_{\theta\theta}$ is the auto-spectral density of $\theta\,(t)$.

As a measure of linearity the coherences for both FT and PT were estimated according to:

$$\hat{\gamma}^2_{FT}(f) = \sqrt{\frac{\left|\hat{G}_{\theta T}(f)\right|^2}{\hat{G}_{\theta\theta}(f)\hat{G}_{TT}(f)}}, \hat{\gamma}^2_{PT}(f) = \sqrt{\frac{\left|\hat{G}_{d\theta}(f)\right|^2}{\hat{G}_{dd}(f)\hat{G}_{\theta\theta}(f)}}$$

By definition the coherence varies between 0 and 1, where 1 indicates that the signals are linearly related and no noise is present. $\hat{\gamma}^2_{FT}$ represents the coherence for the FT and $\hat{\gamma}^2_{PT}$ the coherence for the PT.

All cross-spectral densities used to calculate the FRFs were calculated from an average of ten cross-spectral densities (5 trials $\times$ 2 segments) to reduce the variance. The FRFs and coherences were only evaluated at frequencies where the perturbation signal contained power.

The effective stiffness k_{eff} was calculated from the admittance gain by inverting the average of the 4 lowest frequency points ($< 0.916\%\ Hz$) and served as a measure for the low-frequency behavior of the wrist joint.

Parametric System Identification

The linear wrist model presented in Figure 4 and described in detail in Mugge et al. (2010) and Schouten et al. (2008c) was used to fit the experimentally measured data. The model included the simulated manipulator environment and 10 physiologically interpretable parameters for the human admittance. A total of 9 parameters was fitted for the admittance of which 4 were condition-dependent (muscle visco-elasticity b and k; muscle spindle (MS) velocity feedback k_v; GTO force feedback k_f) and 5 condition-independent (limb inertia m, hand grip dynamics k_c and b_c; neural time delay T_d; eigenfrequency of the muscle activation dynamics F_0). The parameter fit was guided by parameter boundaries (see Appendix Table A.2) and the relative damping of the second-order activation dynamics was fixed to $\beta = 0.7$ to improve convergence. MS length feedback k_p and tendon stiffness k_{se} (represented as H_{tendon} in Figure 4) showed an extremely large standard error of the mean, meaning they could not be estimated reliably and could assume any value. k_p and k_{se} were therefore omitted from the model.

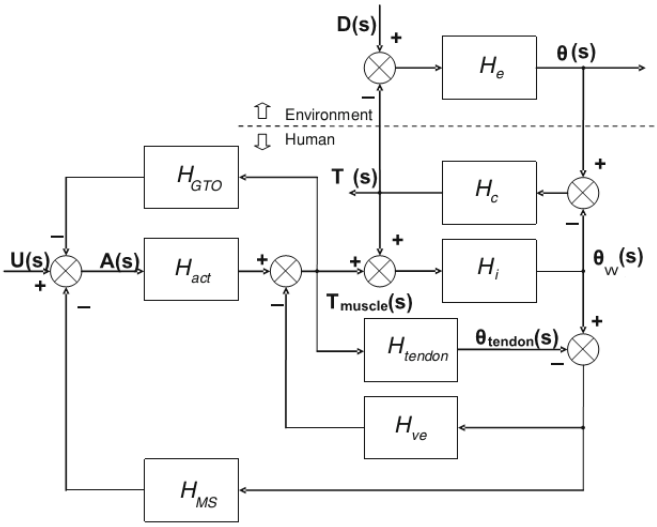

Figure 4: Model of the wrist together with the simulated manipulator environment H_e. The external torque perturbation $D\,(s)$, wrist reaction torque $T\,(s)$, and angle of the handle $\theta\,(s)$ are measured. H_c represents the grip dynamics, H_i intrinsic properties (inertia), H_{ve} muscle visco-elasticity, H_{act} activation dynamics, H_{GTO} force feedback, H_{MS} muscle spindle feedback (only velocity feedback included), H_{tendon} tendon stiffness (set as infinitely stiff) and $\theta_W\,(s)$ the angle of the wrist.

Parameter Fit Procedure

The parameters were quantified by fitting the model H_{Model} FRF onto the spectral FRFs $H_{Spectral}$ grouped for WB and RP conditions. First, a solution for the two PT conditions B00P, B02P was computed. Second, the six RP conditions (PT and FT) were fitted using the condition-independent parameters determined from step 1 as fixed parameters. The parameters were estimated by the following least squares minimization procedure:

$$E = \sum_{cond(1)}^{cond(k)} \sum_{f(1)}^{f(m)} \left| \log \left(\frac{H_{Spectral}}{H_{Model}} \right) \right|^2$$

with $f(1)$ representing the lowest frequency, $f(m)$ the highest, $cond(1)$ the first and $cond(k)$ the last condition fitted.

Model Validation

The quantified parameters were used for forward simulations of the wrist response in the time domain with the model of Figure 4. The PT simulation used the force perturbation signals applied in the experiments as model input and included the environment. The FT simulation used the measured torque exerted on the handle as model input without including the environment. The validity of the quantified parameters is expressed in the variance accounted for (VAF) of the angular position:

$$VAF_\theta = 100 * \left(1 - \frac{\sum_{k=1}^{n} \left| \theta\left(t_k\right) - \hat{\theta}\left(t_k\right) \right|^2}{\sum_{k=1}^{n} \left| \theta\left(t_k\right) \right|^2} \right)$$

in which $\hat{\theta}\left(t_k\right)$ is the simulated handle position, $\theta\left(t_k\right)$ the measured handle position averaged over the five repetitions and n the index of the time vector. A VAF of 100% mean that two signals are equal, lower values indicate that they differ. The first sample was chosen after 1 second to exclude transient effects of integrators (parametric model). VAFs were calculated for each trial segment.

2.4.4 Statistical Analysis

Not all data had equal variances (Levene's test of Homogeneity of Variance) and was normally distributed (Shapiro-Wilk test). M1, M2 obtained from the transient analysis and the 4 condition-dependent model parameters (k, b, k_v and k_f) and the effective stiffness k_{eff} obtained from the continuous analysis were tested for effects of activation level, perturbation bandwidth, damping and task instruction using the non-parametric Friedman and Wilcoxon signed-rank test. An effect of task instruction on $M1$ and $M2$ was tested only by comparing PT/FT pairs with non-significant differences in the flexor background activation since it alone affects the amplitudes of $M1$ and $M2$ (Pruszynski et al. 2009, Toft et al. 1989). The Friedman test was used to identify if an overall difference existed between conditions (test value reported as χ^2) and post-hoc comparisons were done with the Wilcoxon signed-rank (test value reported as Z) to examine where the differences occurred. SPSS 20 was used with a significance level of $p = 0.05$. The error bars in bar plots show the standard deviations of the respective variable for 11 subjects.

3 Results

3.1 MVC

The MVC measurement at the beginning of the experiment yielded the following average maximum voluntary torque over all subjects: 9.52 (SD 4.88) Nm $T_{MVC,flex}$ in flexion and -7.31 (SD 3.12) Nm $T_{MVC,ext}$ in extension direction (values for all subjects are given in Appendix Table C.1).

3.2 Ramp Sequence

A typical example of the flexor EMG (EMG_{flex}) responses to the transient perturbation averaged over 10 repetitions is shown in Figure 1 for a single subject and the three required flexion torque levels (10% (M10R, black), 25% (M25R, dark grey), 40% (M40R, light grey) $T_{MVC,flex}$). The perturbation with a stretch duration of $\sim 67\ ms$ elicited a clear M1 about 25 ms and an M2 about $40 - 50\ ms$ after stretch onset.

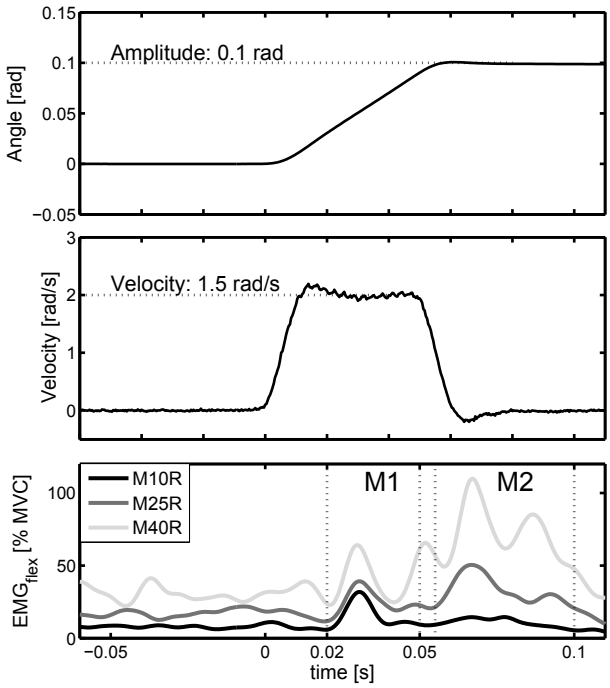

Figure 1: Perturbation characteristics and averaged flexor EMG (EMG_{flex}) responses of one subject shown at three levels of required flexion target torque (10% (M10R, black), 25% (M25R, dark grey), 40% (M40R, light grey) $T_{MVC,flex}$). Top panel: position of the manipulator handle, representing the ramp-and-hold perturbation. Middle panel: velocity of the handle. Bottom panel: EMG_{flex} averaged over 10 ramp-and-hold disturbances for each condition. M1 and M2 amplitudes were determined as the average EMG_{flex} in the fixed time windows of $20 - 50\ ms$ (M1) and $55 - 100\ ms$ (M2).

Increasing flexion torque lead to a significant increase in $M1_{MVC}$ and $M2_{MVC}$ which is illustrated by the average EMG_{flex} response over all subjects in Figure 2 and the statistical results in Table 3.1 (see Appendix Figure C.1 for distributions). On the contrary, the normalized EMG yields an $M1_{BG}$ decreasing with increasing torque level while no significant effect was found for $M2_{BG}$.

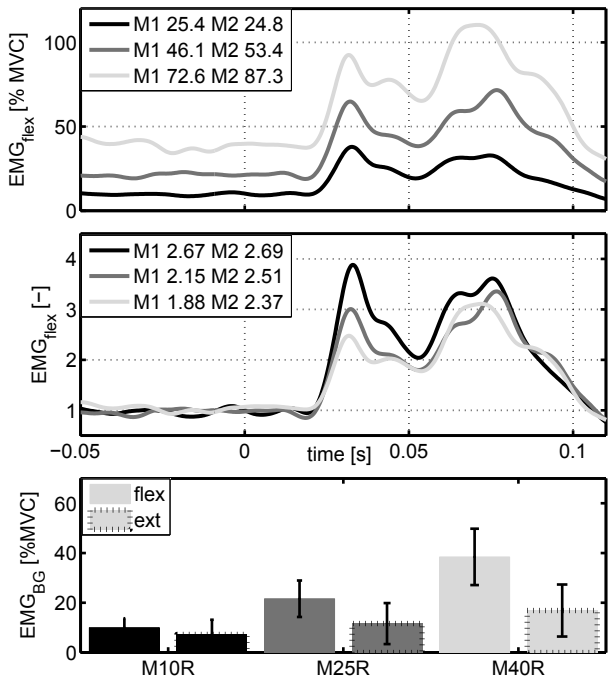

Figure 2: Effect of the flexor activity on the transient response averaged over all subjects (10% (M10R, black), 10% (M25R, dark grey), 25% (M40R, light grey) required flexion target torque $T_{MVC,flex}$). Upper two panels show the flexor EMG (EMG_{flex}) response averaged over all subjects in $\%MVC$ (top) and normalized to flexor background activation (middle). The legends present M1, M2 values in respective units. Bottom panel shows the background activation EMG_{BG} of flexor (solid edges) and extensor muscle (dashed edges) averaged over all subjects and the standard deviation of the subjects EMG_{BG} (error bars).

Table 3.1: Statistical analysis results of the ramp sequence task done at three levels of flexion torque: 10% (M10R), 25% (M25R), 40% (M40R) $T_{MVC,flex}$. Significant comparisons are emphasized in bold letters.

		Medians			M25R/M10R		M40R/M25R	
Variable	Unit	M10R	M25R	M40R	Test value	p	Test value	p
$M1_{BG}$	$[-]$	2.19	2.05	1.84	$Z = -2.134$	**0.032**	$Z = -2.223$	**0.024**
$M1_{MVC}$	$[\%MVC]$	22.75	44.01	65.74	$Z = -2.934$	**0.001**	$Z = -2.934$	**0.001**
$M2_{BG}$	$[-]$	1.96	2.61	2.06	$\chi^2 = 1.273$, $p = 0.629$			
$M2_{MVC}$	$[\%MVC]$	22.19	55.94	84.87	$Z = -2.934$	**0.001**	$Z = -2.934$	**0.001**

3.3 Main Experiment

3.3.1 Position Task

Increasing the external damping (B02P) or reducing the perturbation bandwidth (M00P) resulted in a significant increase in $M2_{MVC}$ without significantly affecting the contraction levels of flexor $EMG_{BG,flex}$ and extensor $EMG_{BG,ext}$ as depicted in the top and bottom panel of Figure 3a and shown by the statistical results in Table 3.2. $M1_{MVC}$, $M1_{BG}$ and $M2_{BG}$ did not show significant effects (see Appendix Figure C.2 for distributions). Joint admittance for low frequencies significantly decreased with increased damping and reduced bandwidth which can be observed from the average admittance over all subjects in the top panel of Figure 3b and from the significant increase in the effective stiffness k_{eff} (statistics in Table 3.2). With damping, the coherence C^2 (bottom panel Figure 3b) was high throughout all frequencies indicating that the external noise was low. Reduced bandwidth showed a high coherence for all frequencies except for mid frequencies starting with a substantial drop at the first frequency of reduced power $\sim 1.7\ Hz$ up to $\sim 10\ Hz$. Coherence for the wide-bandwidth perturbation without damping (B00P) was especially low for low frequencies, increasing towards higher frequencies with a dip around the eigenfrequency.

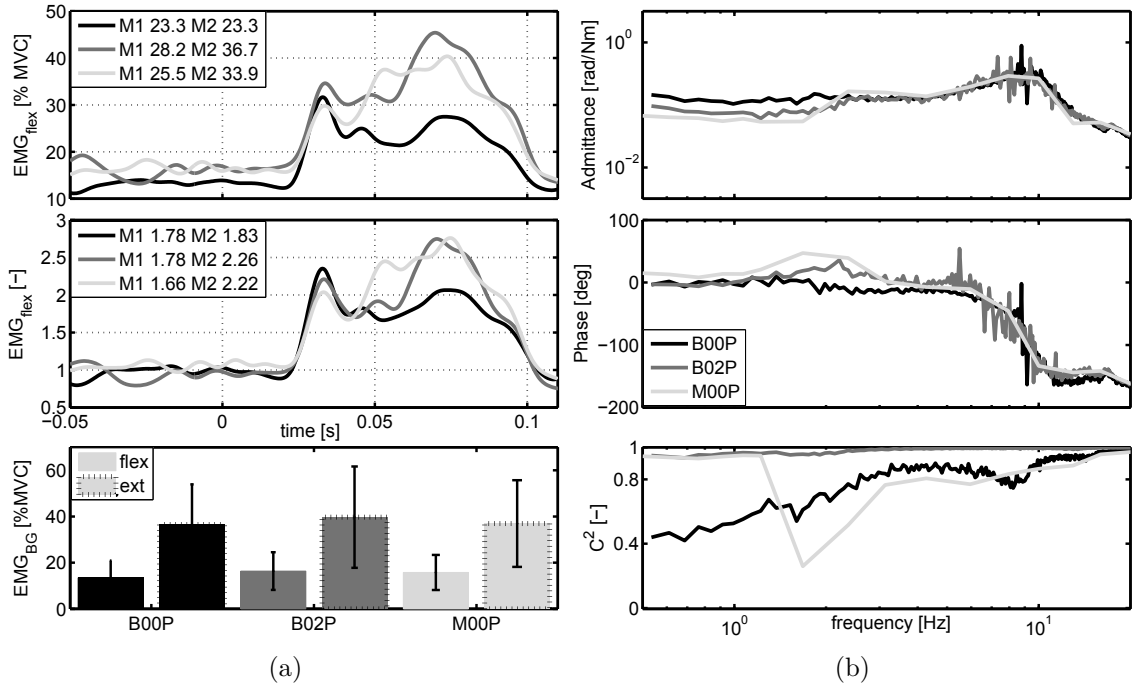

(a) (b)

Figure 3: Damping and perturbation bandwidth effect on the transient response and admittance averaged over all subjects (no damping (B00P, black), 2 Nms/rad damping (B02P, dark grey), reduced bandwidth (M00P, light grey)). 3a) Upper two panels show the average flexor EMG (EMG_{flex}) response in $\%MVC$ (top) and normalized to flexor background activation (middle). The legend presents M1, M2 values in respective units. The bottom panel shows the EMG_{BG} of flexor (solid edges) and extensor muscle (dashed edges) averaged over all subjects and the standard deviation of the subjects EMG_{BG} (error bars). 3b) Admittance with the magnitude (top -), phase (middle -) and coherence-squared C^2 (bottom panel).

Table 3.2: Statistical analysis results of the position task conditions: no damping (B00P), 2 Nms/rad damping (B02P), reduced perturbation bandwidth (M00P). Significant comparisons are emphasized in bold letters.

		Medians			B02P/B00P		M00P/B00P	
Variable	Unit	B00P	B02P	M00P	Test value	p	Test value	p
$M1_{BG}$	$[-]$	1.68	1.74	1.63	$\chi^2 = 2.36, p = 0.351$			
$M1_{MVC}$	$[\%MVC]$	26.18	27.74	28.99	$\chi^2 = 4.55, p = 0.116$			
$M2_{BG}$	$[-]$	1.59	2.38	1.93	$\chi^2 = 3.46, p = 0.219$			
$M2_{MVC}$	$[\%MVC]$	20.82	34.53	33.17	$Z = -2.934$	**0.001**	$Z = -2.934$	**0.001**
$EMG_{BG,flex}$	$[\%MVC]$	15.25	14.34	17.47	$\chi^2 = 3.82, p = 0.163$			
$EMG_{BG,ext}$	$[\%MVC]$	33.42	33.99	31.51	$\chi^2 = 2.36, p = 0.351$			
k_{eff}	$[Nm/rad]$	8.61	12.33	16.34	$Z = -2.934$	**0.001**	$Z = -2.934$	**0.001**

Parametric System Identification

Figure 4 depicts a typical example of the fit in time for one subject. The VAFs were high (lowest score 72% (SD 12.3) M00P) for all three conditions indicating that the model described the observed mechanical behavior well (see Table 3.3).

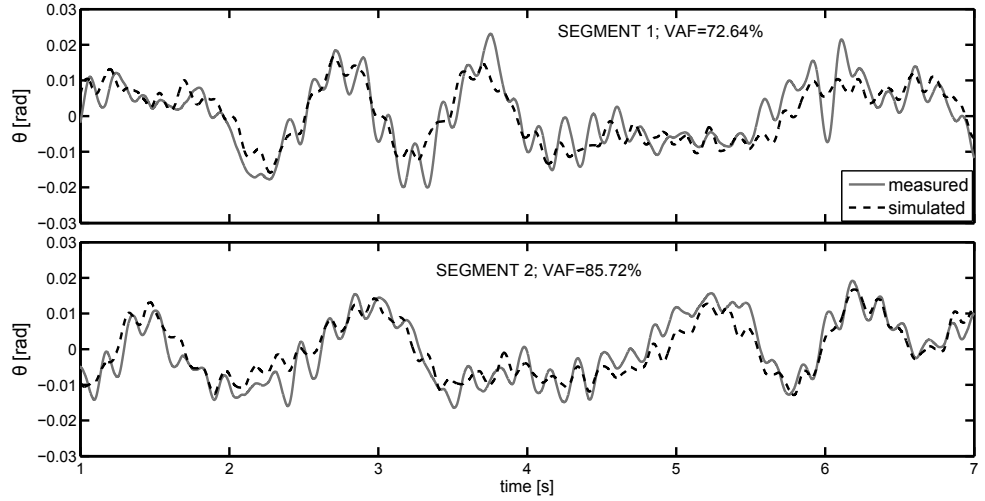

Figure 4: Example of the forward simulation of the handle position for one subject during the reduced perturbation bandwidth condition (M00P). 6 s of entire 13.1 s used for identification shown for the two segments within a trial.

Table 3.3: VAF values for PT conditions: no damping (B00P), damping (B02P), reduced bandwidth (M00P). Means (SD) in % over the 11 subjects given for the two segments within a trial.

	B00P	B02P	M00P
Segment 1	85.5 (6)	90.5 (4.5)	73.2 (8.8)
Segment 2	87.6 (8.6)	91.3 (2.3)	72 (12.3)

The condition-dependent parameters were both significantly affected by the increased damping (B02P) and reduced perturbation bandwidth (M00P): velocity feedback k_v increased while force feedback k_f decreased, both representing an increase in excitatory reflex feedback (see statistics in Table 3.4). Figure 5 emphasizes this increase in excitatory reflex feedback along with the significant increase in $M2_{MVC}$. The intrinsic stiffness k increased only significantly with reduced perturbation bandwidth. The results for the condition-independent parameters (limb inertia,

hand grip dynamics, neural time delay and muscle activation dynamics eigenfrequency) are comparable with results from previous studies (Mugge 2011, Schouten 2004) using this neuromuscular model (values presented in Appendix Table C.2, distributions in Appendix Figure C.4).

Table 3.4: Statistical analysis results for the condition-dependent parameters intrinsic stiffness k and viscosity b, velocity k_v and force feedback k_f of the position task conditions: no damping (B00P), 2 Nms/rad damping (B02P), reduced bandwidth (M00P). Significant comparisons are emphasized in bold letters.

		Medians			B02P/B00P		M00P/B00P	
Variable	Unit	B00P	B02P	M00P	Test value	p	Test value	p
k	$[Nm/rad]$	11.02	11.52	12.39	$Z = -1.689$	0.102	$Z = -2.845$	**0.002**
b	$[Nms/rad]$	0.037	0.048	0.032	$Z = -2.934$	**0.001**	$Z = -1.245$	0.24
k_v	$[Nms/rad]$	0.02	1.11	1.19	$Z = -2.934$	**0.001**	$Z = -2.667$	**0.005**
k_f	$[-]$	0	-0.36	-0.81	$Z = -2.756$	**0.003**	$Z = -2.934$	**0.001**

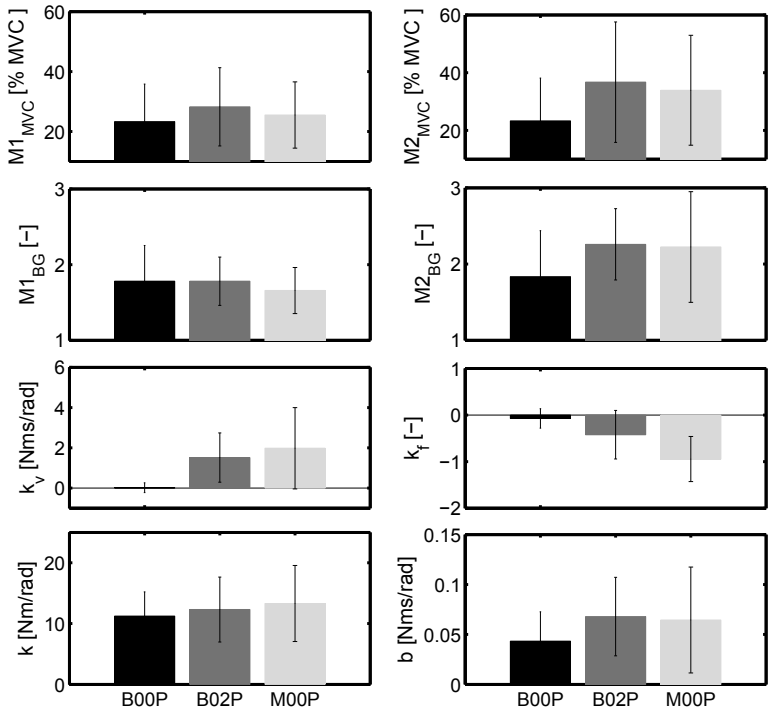

Figure 5: Damping and perturbation bandwidth effect on the transient parameters $M1$ and $M2$ and the condition-dependent parameters obtained from the continuous analysis (no damping (B00P, black), 2 Nms/rad damping (B02P, dark grey), reduced bandwidth (M00P, light grey)). Upper two panels show $M1$ and $M2$ in $\%MVC$ and normalized to flexor background activation. Bottom two panels show the condition-dependent parameters intrinsic stiffness k and viscosity b, velocity k_v and force feedback k_f obtained from the neuromuscular model. The error bars show the standard deviations of the respective variable for all subjects.

3.3.2 Position and Force Task

An effect of task instruction on the low-frequency behavior of the admittance can be seen in Figure 6b which is confirmed by a significantly higher k_{eff} in the PT compared to FT for PT/FT pairs matching in bias torque $\%T_{MVC,flex}$ (see statistics in Table 3.5). The coherence for the FT conditions was low, especially for higher frequencies. Such a low coherence indicates the presence of external noise and that the relation between joint torque and angle is not as linear. The three combinations of M10F/M00P, M25F/M10P and M25F/M25P fulfilled the criteria of a non-significant difference in $EMG_{BG,flex}$ for testing the task effect on $M1$ and $M2$ (see Table 3.5b). Examining the low-frequency admittance of these PT/FT pairs still showed a higher effective stiffness during the PT so an effect of task is also present in these combinations. $M1_{BG}$ is significantly larger during the FT for all three PT/FT pairs while $M1_{MVC}$ is only larger when comparing M25F/M10P. $M2_{BG}$ is lower in the FT for the two pairs M25F/M10P and M25F/M25P while $M2_{MVC}$ is lower for all three comparisons. A significantly higher extensor activation $EMG_{BG,ext}$ in the PT was found for all the three PT/FT pairs, indicating a higher amount of co-contraction.

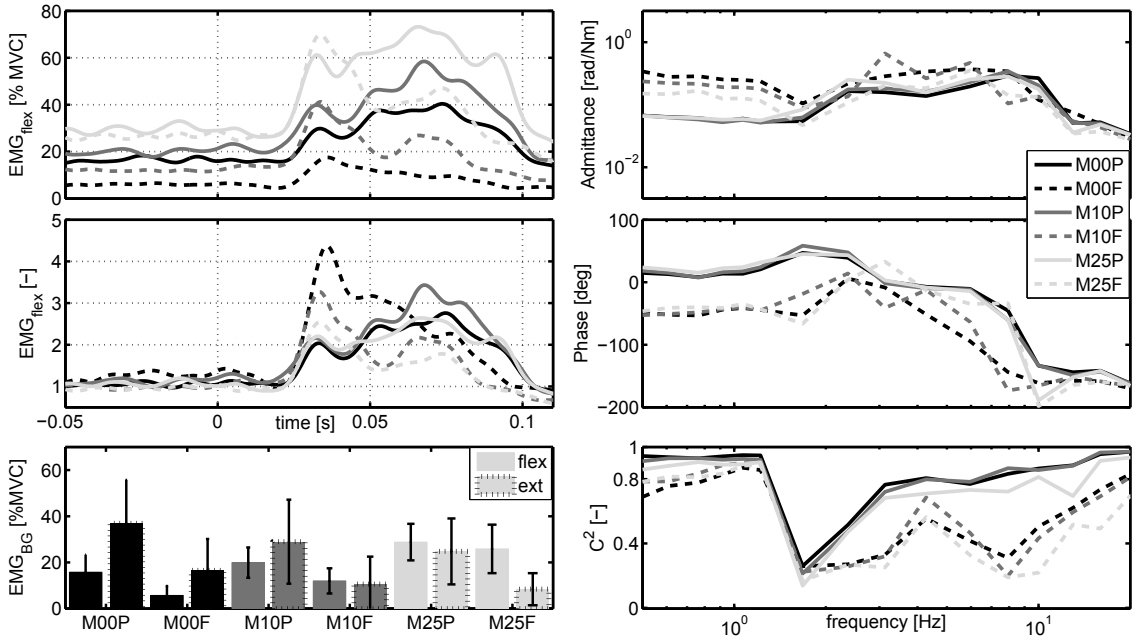

(a) (b)

Figure 6: Task and activation level effect on the transient response and admittance averaged over all subjects (M00P/M00F 0% (black), M10P/M10F 10% (dark grey), M25P/M25F 25% (light grey) $T_{MVC,flex}$ bias torque; PT (solid traces) FT (dotted traces)). 6a) Upper two panels show the average flexor EMG (EMG_{flex}) response in $\%MVC$ (top) and normalized to flexor background activation (middle). Bottom panel shows the EMG_{BG} of flexor (solid edges) and extensor muscle (dashed edges) averaged over all subjects and the standard deviation of the subjects EMG_{BG} (error bars). 6b) Admittance with the magnitude (top -), phase (middle -) and coherence-squared C^2 (bottom panel).

Table 3.5: Statistical analysis results of the position task and force task conditions: M00P/M00F 0%, M10P/M10F 10%, M25P/M25F 25% $T_{MVC,flex}$ bias torque.

(a) Median values of all tested variables in PT/FT.

		Medians					
Variable	Unit	M00P	M10P	M25P	M00F	M10F	M25F
k_{eff}	$[Nm/rad]$	16.34	15.75	16.1	3.22	3.73	5.87
$EMG_{BG,flex}$	$[\%\ MVC]$	17.47	18.37	27.8	5.73	10.94	20.7
$EMG_{BG,ext}$	$[\%\ MVC]$	31.51	27.56	27.38	10.48	8.6	6.56
$M1_{BG}$	$[-]$	1.63	1.75	1.77	2.24	2.08	1.96
$M1_{MVC}$	$[\%\ MVC]$	28.99	34.18	49.83	13.63	21.97	49.83
$M2_{BG}$	$[-]$	1.93	2.31	2.31	1.56	1.48	1.47
$M2_{MVC}$	$[\%\ MVC]$	33.17	43.27	59.74	8.1	14.66	36.3

(b) Test values and significance levels p of all comparisons done for k_{eff}, $EMG_{BG,flex}$ and $EMG_{BG,ext}$. Last three PT/FT pairs separated by horizontal line emphasize conditions with non-significant differences in $EMG_{BG,flex}$. Significant comparisons are emphasized in bold letters.

	k_{eff}		$EMG_{BG,flex}$		$EMG_{BG,ext}$	
Comparison	Test value	p	Test value	p	Test value	p
M00F/M00P	$Z = -2.934$	**0.001**	$Z = -2.934$	**0.001**	-	-
M10F/M10P	$Z = -2.934$	**0.001**	$Z = -2.934$	**0.001**	-	-
M25F/M25P	$Z = -2.934$	**0.001**	$Z = -1.511$	0.147	$Z = -2.934$	**0.001**
M10F/M00P	$Z = -2.934$	**0.001**	$Z = -1.6$	0.123	$Z = -2.934$	**0.001**
M25F/M10P	$Z = -2.934$	**0.001**	$Z = -1.867$	0.067	$Z = -2.934$	**0.001**

(c) Test values and significance levels p for comparisons of PT/FT pairs with non-significant differences in $EMG_{BG,flex}$ for variables: $M1_{BG}$, $M1_{MVC}$, $M2_{BG}$ and $M2_{MVC}$. Significant comparisons are emphasized in bold letters.

	$M1_{BG}$		$M1_{MVC}$		$M2_{BG}$		$M2_{MVC}$	
Comparison	Test value	p	Test value	p	Test value	p	Test value	p
M10F/M00P	$Z = -2.401$	**0.014**	$Z = -0.711$	0.52	$Z = -1.245$	0.24	$Z = -2.401$	**0.014**
M25F/M10P	$Z = -2.045$	**0.042**	$Z = -2.578$	**0.007**	$Z = -2.934$	**0.001**	$Z = -2.578$	**0.007**
M25F/M25P	$Z = -2.667$	**0.005**	$Z = -0.267$	0.831	$Z = -2.934$	**0.001**	$Z = -2.934$	**0.001**

Parametric System Identification

A stable set of parameters for all the conditions in the PT/FT could only be obtained for 2/11 subjects. The parameter estimation for the PT/FT are omitted from the results since 14 unstable solutions were distributed over 9 subjects. A table of the VAF values for all subjects and PT/FT conditions is given in the Appendix C.3.

4 Discussion

With the position task, the joint admittance decreased with damping provided by the environment as well as with reduced perturbation bandwidth, both in accordance with previous studies (Mugge 2011, Schouten 2004). Consistent with Mugge (2011), the task instruction "minimize force deviations" increased the joint admittance with respect to the instruction "minimize displacements". However, the transient responses M1 and M2 did not behave as hypothesized since the thought changes in M1 with damping, perturbation bandwidth and task instruction were found in M2. Furthermore, M1 normalized to background activity was found to be detrimental to task-performance as a larger response was found in the FT than in the PT.

Motor adaptations to changes in environment and perturbation bandwidth

Increased damping (B02P) and reduced bandwidth (M00P) in the PT significantly increased the long-latency response M2 while it did not affect the short-latency response M1. Agonist contraction level (Pruszynski et al. 2009, Toft et al. 1989) and co-contraction of agonist and antagonist (Nielsen et al. 1994) which are known to influence M1 and M2 magnitudes were ruled out as potential sources of modulation since no significant changes in the flexor and extensor activation were found between the PT conditions B00P, B02P and M00P. The M2 in the FCR has previously been linked to muscle spindle (MS) Ia afferents, mainly providing muscle velocity - but also muscle length feedback and II afferents, mainly conducting muscle length information (Kandel et al. 2000, Meskers et al. 2010). The neuromuscular model yielded increased excitatory velocity k_v and force feedback k_f during the increased damping and reduced bandwidth conditions. An increase in velocity feedback k_v could represent an increase in the MS afferent's velocity sensitivity which can be adjusted by the central nervous system (CNS) through primarily presynaptic inhibition and activation of γ-'dynamic' motoneurons, yet no increase in M1 was found (Kandel et al. 2000). Ib afferents, transmitting force feedback from GTOs, are from the same fast fiber group as Ia afferents and are connected to α-motoneurons of the same muscle via one inhibitory interneuron (Kandel et al. 2000). Therefore, an increase in excitatory k_f could be reflected in the short-latency response M1. However, studies relating force feedback from GTOs to the short- and long-latency stretch reflex responses M1 and M2 are sparse. Excitatory force feedback has been shown during human walking by Grey et al. (2007) based on decreased EMG responses $30-80\ ms$ after the onset of ankle perturbations which is somewhere in between the latencies of M1 and M2. How excitatory force feedback would manifest itself in the context of a posture task at the wrist is not known. The increase in M2 could be explained by increased II afferent feedback but the link to the neuromuscular model cannot be made based on results from this study since k_p was omitted. Yet, a major role for k_p in the observed modulation is unlikely judging from Schouten (2004) who reported only little contribution from length feedback during the PT and only little modulation with damping. Other possible explanations for the modulation of M2 are presynaptic inhibition which affects the transmission from afferents to motoneurons by decreasing or increasing the synaptic effectiveness or transcortical pathways where afferent pathways are affected by neurons descending from the CNS (Ludvig et al. 2007, MacKinnon et al. 2000).

"Automatic Gain-Scaling" in the ramp sequence task

During the ramp sequence task M1 and M2 in % MVC both significantly increased with the required flexion torque. When normalized to background activity M1 decreased while the normalized M2 did not show a significant effect, rather maintaining a steady level (see Appendix Figure C.1). The behavior of M1 and M2 observed in the ramp sequence task are in line with findings by Toft et al. (1989) who used ramp-and-hold displacements and a "do not intervene" instruction at contraction levels up to 80% MVC torque. This behavior is considered controversial since it goes against the well-established phenomenon called "Automatic Gain-Scaling" in which the EMG response evoked by a perturbation increases progressively with the level of background activity and so remains an approximate constant proportion of the background activity (Pruszynski et al. 2009). This phenomenon, generally attributed to the "size recruitment principle" where motor units are recruited in the order of their force-generating capabilities, is typically seen for the short-latency response M1 and has been reported to start decreasing within the long-latency period for elbow muscles ($\sim 75\ ms$) (Pruszynski et al. 2009). Why M1 disobeys the "Automatic Gain-Scaling" which is commonly seen in upper-limb muscles in the ramp sequence task remains unknown.

Motor adaptation to task instruction

The effect of task instruction on the behavior of the low-frequency admittance could not be linked to the neuromuscular parameters but was consistent with Mugge (2011) who found decreased excitatory (position and velocity feedback) and increased inhibitory reflexive feedback (force feedback). Assuming that k_p represents II -, k_v Ia - and k_f Ib afferent feedback and that these gains behaved as in Mugge (2011) one would expect M1 and M2 to be decreased in the FT. Nevertheless, only M2 significantly decreased during the FT with respect to the PT ($M2_{MVC}$ 3/3 PT/FT pairs, $M2_{BG}$ 2/3 PT/FT pairs) and interestingly counterproductive to the task M1 was larger during the FT ($M1_{MVC}$ 1/3 PT/FT pairs, $M1_{BG}$ 3/3 PT/FT pairs). The M2 behavior confirms previous results by Doemges & Rack (1992) who used continuous random perturbations (3 sines with frequencies $<0.3\ Hz$) with ramp-and-hold displacements but only focused on the transient responses. In Doemges & Rack (1992) as well as in this study co-contraction was found in the PT which lies in the nature of the task, since co-contraction increases joint stiffness and is as such an effective way to minimize displacements. To eliminate antagonist activation and ensure that the observed differences in reflexes are only due to changes in task instruction, Doemges & Rack (1992) anaesthetized the antagonist whereas the current study introduced bias forces onto the agonist. The influence of background activation on M1 and M2 was controlled by only comparing PT/FT conditions with matching agonist activation but higher antagonist activation remained in the PT which still leaves co-contraction as a potential influence on the observed transient response. Nielsen et al. (1994) investigated M1 under different levels of co-contraction at the ankle and found that on average M1 was larger during co-contraction at matched levels of ankle flexion. Evidence from other studies by Nielsen suggest that the increase in M1 during co-contraction is due to depressed reciprocal inhibition of Ia inhibitory interneurons connected to antagonist muscles leading to higher excitability of motoneurons (Nielsen & Kagamihara 1992) and despite increased presynaptic inhibition (Nielsen & Kagamihara 1993). Pierrot-Desseilligny & Burke (2005) however, cite the results by Nielsen et al. (1994) with:"the stretch reflex is reduced during weak, and mainly unchanged during strong co-contractions (Nielsen et al. 1994)" and thereby refers to

results specific to groups of subjects. Results by Nielsen et al. (1994) demonstrate that co-contraction affects M1, how exactly remains unclear though. Furthermore, conclusions from Nielsen et al. (1994) have to be made with caution since physiological differences exist between the ankle and the wrist joint (Pierrot-Desseilligny & Burke 2005). Another factor definitely affecting the transient response is the different afferent input provided in both tasks, the pre-filtered RP position perturbation used in the FT resulted in lower velocities at the wrist than the non-filtered RP force perturbation in the PT. A silent period of 100 ms of zero velocity and position was introduced before every ramp-and-hold stretch to wait for the motoneurons refractory period to pass. The duration of the silent period was determined from pilot experiments and ensured that a clear M1 was elicited by the ramp-and-hold perturbation. However, the exact effect of the silent period duration together with changes in afferent firing caused by different continuous perturbation frequency content on the M1 is unknown. Furthermore, Stein & Kearney (1995) demonstrated that muscle shortening preceding the stretch perturbation decreased M1 depending on the timing of the preceding shortening with effects lasting for as long as 1 s. The results from Stein & Kearney (1995) emphasize the direct impact of stretch history on transient responses which leaves an uncertainty on the observed behavior of M1 since different tasks and conditions in this study also implicate changes in afferent input.

M1, M2 and the fitted neuromuscular parameters

The estimated neural time delay T_d 26.6 (SD 10.8) ms together with the assumptions that k_v represents feedback from Ia - and k_f from Ib afferents suggest that the reflex modulation observed from the continuous perturbations stems from short-latency pathways. However, the M1 and M2 behavior from this study does not support the inference made from the neuromuscular model that modulation stems from short-latency pathways instead modulation does take place at longer-latency. How the pathways constituting M1 and M2 are in effect during the continuous perturbation is not known but short- and long-latency pathway firing can be expected to be overlapping in time. The reflexive time delay fitted by the model represents an effective time delay best describing the joint contributions of the I and II afferents. Speculatively, the contribution of the stereotyped short latency response biases the estimated time delay of the modulating long latency response. The underestimated time delay of the modulating feedback may easily be interpreted as too low for long latency. Reflex gains from the neuromuscular model are derived from the observed mechanical behavior on the joint level and reflect the mechanical contribution of a reflex pathway to the output force. Physiological processes such as MS dynamics, γ-activation and presynaptic inhibition that have direct influence on the amplitudes of M1 and M2 derived from the measured muscle activation, are lumped into the reflex gains. Reflex gains are also determined under the assumption of linearity with small perturbations around an operating point which is certainly not satisfied by the large ramp-and-hold displacements used to elicit M1 and M2 (Stein & Kearney 1995). Furthermore, M1 and M2 represent a uni-directional measure for reflexes while the neuromuscular reflex gains combine agonist and antagonist interactions. The results obtained in this study do not allow a conclusive determination of the source of modulation mainly observed in M2. Results indicate that the continuous approach did not condition M1 as hypothesized and that the reflexive feedback from short-latency pathways (velocity and force feedback) obtained via the presented neuromuscular model does not directly map to the M1 elicited by ramp-and-hold perturbations.

5 Conclusion

- In line with (Mugge 2011, Schouten 2004), increased external damping or reduced continuous perturbation bandwidth in a position task did result in a decreased joint admittance and increased excitatory reflexive feedback, especially velocity and force feedback.
- Increased external damping or reduced continuous perturbation bandwidth in a position task did result in an increase in M2, while no effect on M1 was found.
- In line with (Mugge 2011), task-instruction affected the joint admittance. The force task did yield an increased joint admittance with respect to the position task. The admittance behavior in force and position task with bias forces could not be linked to neuromuscular parameters, since they did not consistently converge.
- Task-instruction affected both M1 and M2. M2 was found to be significantly decreased during the force task consistent with the admittance behavior while M1 normalized to background activation was found to be increased.
- The continuous perturbations along with the mechanical environment did not condition M1 as hypothesized, adding to the range of paradigms for which a stereotyped M1 has been demonstrated.
- Furthermore, results indicate that reflexive velocity and force feedback obtained via the presented neuromuscular model does not directly map to the M1 elicited by brief ramp-and-hold perturbations.

References

Corden, D. & Lippold, O. (2000), 'Long-latency component of the stretch reflex in human muscle is not mediated by intramuscular stretch receptors', *Journal of Neurophysiology* **84**, 184.

De Vlugt, E., Schouten, A. C. & Van Der Helm, F. C. T. (2002), 'Adaptation of reflexive feedback during arm posture to different environments.', *Biological Cybernetics* **87**, 10–26.

Doemges, F. & Rack, P. M. (1992), 'Task-dependent changes in the response of human wrist joints to mechanical disturbance.', *The Journal of Physiology* **447**, 575–585.

Grey, M. J., , Nielsen, J. B., N, M. & Sinkjaer, T. (2007), 'Positive force feedback in human walking', *The Journal of Physiology* **581**, 99–105.

Grey, M. J., Ladouceur, M., Andersen, J. B., Nielsen, J. B. & Sinkjaer, T. (2001), 'Group II muscle afferents probably contribute to the medium latency soleus stretch reflex during walking in humans.', *The Journal of Physiology* **534**, 925–33.

Kandel, E., Schwartz, J. & Jessell, T. (2000), *Principles of neural science*, Vol. 3, McGraw-Hill.

Kearney, R. E., Stein, R. B. & Parameswaran, L. (1997), 'Identification of intrinsic and reflex contributions to human ankle stiffness dynamics.', *IEEE transactions on biomedical engineering* **44**, 493–504.

Kurtzer, I. L., Pruszynski, J. A. & Scott, S. H. (2008), 'Long-latency reflexes of the human arm reflect an internal model of limb dynamics.', *Current biology.* **18**, 449–53.

Kurtzer, I., Pruszynski, J. A. & Scott, S. H. (2010), 'Long-latency and voluntary responses to an arm displacement can be rapidly attenuated by perturbation offset.', *Journal of Neurophysiology* **103**, 3195–204.

Lewis, G. N., MacKinnon, C. & Perreault, E. J. (2006), 'The effect of task instruction on the excitability of spinal and supraspinal reflex pathways projecting to the biceps muscle', *Experimental Brain Research* **174**, 413–425.

Ludvig, D., Cathers, I. & Kearney, R. E. (2007), 'Voluntary modulation of human stretch reflexes', *Experimental Brain Research* **183**, 201–213.

MacKinnon, D., Verrier, M. & Tatton, W. (2000), 'Motor cortical potentials precede long-latency EMG activity evoked by imposed displacements of the human wrist', *Experimental Brain Research* **131**, 477–490.

Meskers, C. G. M., Schouten, A. C., Rich, M. M. L., De Groot, J. H., Schuurmans, J. & Arendzen, J. H. (2010), 'Tizanidine does not affect the linear relation of stretch duration to the long latency M2 response of m. flexor carpi radialis', *Experimental Brain Research* **201**, 681–688.

Mugge, W. (2011), Reflex mechanisms in CRPS-related dystonia, PhD thesis, Delft University of Technology, Delft, The Netherlands.

Mugge, W. & Abbink, D. A. (2007), 'Reduced power method: how to evoke low-bandwidth behaviour while estimating full-bandwidth dynamics', *Robotics, 2007. ICORR* .

Mugge, W., Abbink, D. A., Schouten, A. C., Dewald, J. P. A. & Van Der Helm, F. C. T. (2010), 'A rigorous model of reflex function indicates that position and force feedback are flexibly tuned to position and force tasks', *Experimental Brain Research* **200**, 325–340.

Nielsen, J. & Kagamihara, Y. (1992), 'The regulation of disynaptic reciprocal Ia inhibition during co-contraction of antagonistic muscles in man', *Journal of Physiology* **456**, 373–391.

Nielsen, J. & Kagamihara, Y. (1993), 'The regulation of presynaptic inhibition during co-contraction of antagonistic muscles in man', *Journal of Physiology* **464**, 575–593.

Nielsen, J., Sinkjaer, T. & Kagamihara, Y. (1994), 'Segmental reflexes and ankle joint stiffness during co-contraction of antagonistic ankle muscles in man', *Experimental Brain Research* **102**, 350–358.

Pierrot-Desseilligny, E. & Burke, D. C. (2005), *The circuitry of the human spinal cord: its role in motor control and movement disorders*, Cambridge University Press.

Pintelon, R. & Schoukens, J. (2001), *System Identification. A frequency domain Approach*, IEEE Press.

Pruszynski, J. A., Kurtzer, I., Lillicrap, T. P. & Scott, S. H. (2009), 'Temporal Evolution of "Automatic Gain-Scaling"', *Journal of Neurophysiology* **102**, 992–1003.

Pruszynski, J. A., Kurtzer, I. & Scott, S. H. (2008), 'Rapid motor responses are appropriately tuned to the metrics of a visuospatial task.', *Journal of Neurophysiology* **100**, 224–238.

Schouten, A. C. (2004), Proprioceptive reflexes and neurological disorders, PhD thesis, Delft University of Technology, Delft, The Netherlands.

Schouten, A. C., De Vlugt, E. & Van Der Helm, F. C. T. (2008a), 'Design of perturbation signals for the estimation of proprioceptive reflexes', *IEEE Transactions on Biomedical Engineering* **55**, 1612–1619.

Schouten, A. C., De Vlugt, E., Van Hilten, B. J. J. & Van Der Helm, F. C. T. (2006), 'Design of a torque-controlled manipulator to analyse the admittance of the wrist joint.', *Journal of Neuroscience Methods* **154**, 134–141.

Schouten, A. C., Mugge, W. & Van Der Helm, F. C. T. (2008c), 'NMClab, a model to assess the contributions of muscle visco-elasticity and afferent feedback to joint dynamics.', *Journal of Biomechanics* **41**, 1659–1667.

Schuurmans, J., De Vlugt, E., Schouten, A. C., Meskers, C. G. M., de Groot, J. H. & van der Helm, F. C. T. (2009), 'The monosynaptic Ia afferent pathway can largely explain the stretch duration effect of the long latency M2 response.', *Experimental Brain Research* **193**, 491–500.

Shemmell, J., Krutky, M. A. & Perreault, E. J. (2010), 'Stretch sensitive reflexes as an adaptive mechanism for maintaining limb stability.', *Clinical Neurophysiology* **121**, 1680–9.

Stein, R. & Kearney, R. (1995), 'Nonlinear behavior of muscle reflexes at the human ankle joint', *Journal of Neurophysiology* **73**, 65–72.

Toft, E., Sinkjaer, T. & Andreassen, S. (1989), 'Mechanical and electromyographic responses to stretch of the human anterior tibial muscle at different levels of contraction', *Experimental Brain Research* **74**, 213–219.

Van Der Helm, F. C. T., Schouten, A. C., De Vlugt, E. & Brouwn, G. G. (2002), 'Identification of intrinsic and reflexive components of human arm dynamics during postural control.', *Journal of Neuroscience Methods* **119**, 1–14.

Appendix

A Supplementary Tables - Method

Table A.1: Parameters used for the reduced power position perturbation filter

Parameter	Description	Value	Unit
m	Hand inertia	0.0026	kgm^2
b_c	Grip viscosity	1.35	Nms/rad
k_c	Grip stiffness	59.6	Nm/rad
k_{se}	Tendon stiffness	967.9	Nm/rad
F_0	Activation dynamics eigenfrequency	2.1	Hz
β	Activation dynamics relative damping	1.28	–
T_d	Neural time delay	0.03	s
b	Muscle viscosity	0.023	Nms/rad
k	Muscle stiffness	1.66	Nm/rad
k_p	MS length feedback	-0.1	Nm/rad
k_v	MS velocity feedback	0.005	Nms/rad
k_f	GTO force feedback	1.51	–

Table A.2: Parameter Boundaries

Parameter	Description	Lower boundary	Upper boundary	Unit
m	Hand inertia	0.0001	0.0006	kgm^2
b_c	Grip viscosity	0.01	5	Nms/rad
k_c	Grip stiffness	1	300	Nm/rad
F_0	Activation dynamics eigenfrequency	0.5	10	Hz
T_d	Neural time delay	0.015	0.05	s
b	Muscle viscosity	0.001	1	Nms/rad
k	Muscle stiffness	0	30	Nm/rad
k_v	MS velocity feedback	-10	10	Nms/rad
k_f	GTO force feedback	-10	10	–

B Transition from continuous to transient perturbations

The transition procedure is depicted in Figure B.1

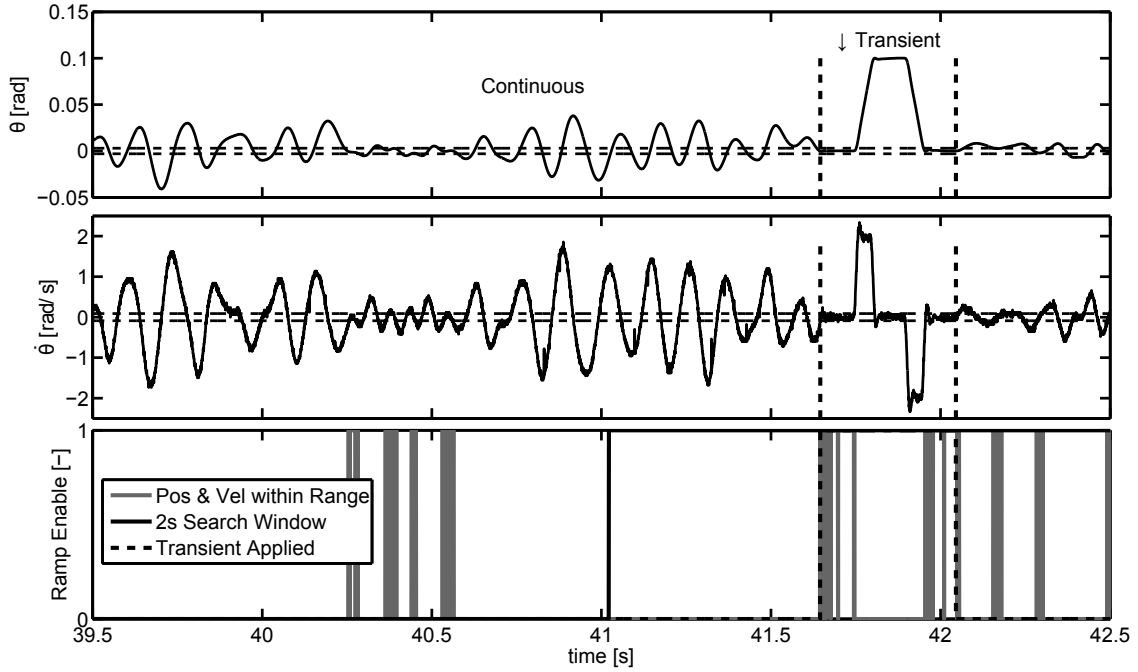

Figure B.1: Transition from continuous to transient perturbation. Transient perturbations were only applied when wrist movements were small ($\theta < |0.003|\ rad$ and $\dot{\theta} < |0.0873|\ rad/s$, each marked with two dashed horizontal lines in the respective figure). A 2 s search window was used to find an instant when both criteria were fulfilled which initiated the transient perturbation.

C Supplementary Results

MVC

Table C.1: Maximum voluntary torques (in Nm) obtained from the 11 subjects for flexion and extension direction at the beginning (subscript 1) and end of the experiment (subscript 2). $T_{MVC,flex1}$ was used to compute the bias force levels applied in the position task and the target force levels required in the ramp sequence task and the force task.

Subject	$T_{MVC,flex1}$	$T_{MVC,flex2}$	$T_{MVC,ext1}$	$T_{MVC,ext2}$
1	14.07	14.17	-9.43	-7.98
2	6.2	5.45	-5	-4.43
3	9.71	9.57	-7.3	-9.13
4	16.41	17.28	-11.41	-12.25
5	3.74	3.64	-3.46	-3.09
6	17.48	18.52	-10.75	-12.99
7	11.08	10.72	-8.93	-8.76
8	10.56	10.89	-10.88	-10.03
9	4.1	5.05	-3.02	-3.82
10	5.43	4.76	-4.81	-5.27
11	5.95	6.33	-5.37	-4.7

Ramp Sequence

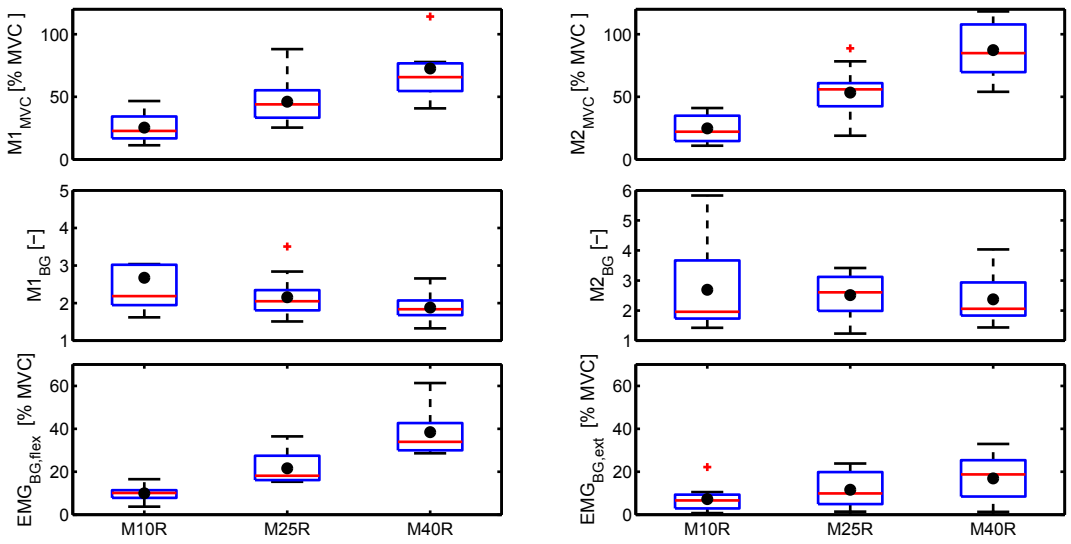

Figure C.1: Ramp sequence. M1, M2 in $\%MVC$ or normalized to $EMG_{BG,flex}$ and the background activation of flexor ($EMG_{BG,flex}$) and extensor carpi radialis ($EMG_{BG,ext}$). Mean values shown as black dot.

Main Experiment

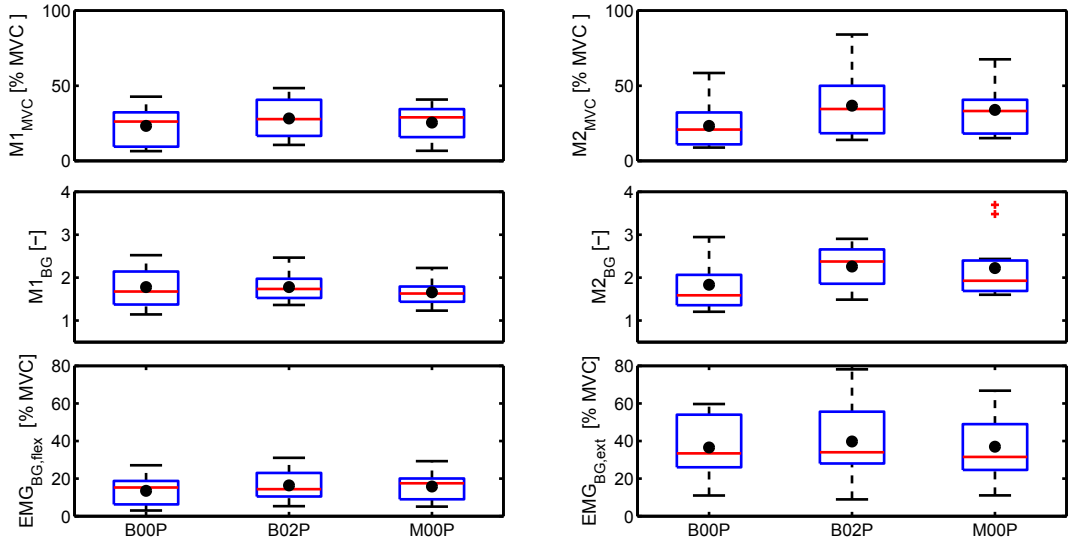

Figure C.2: PT conditions - 11 subjects. M1, M2 in $\%MVC$ or normalized to $EMG_{BG,flex}$ and the background activation of flexor (FCR) and extensor carpi radialis (ECR). Mean values shown as black dot.

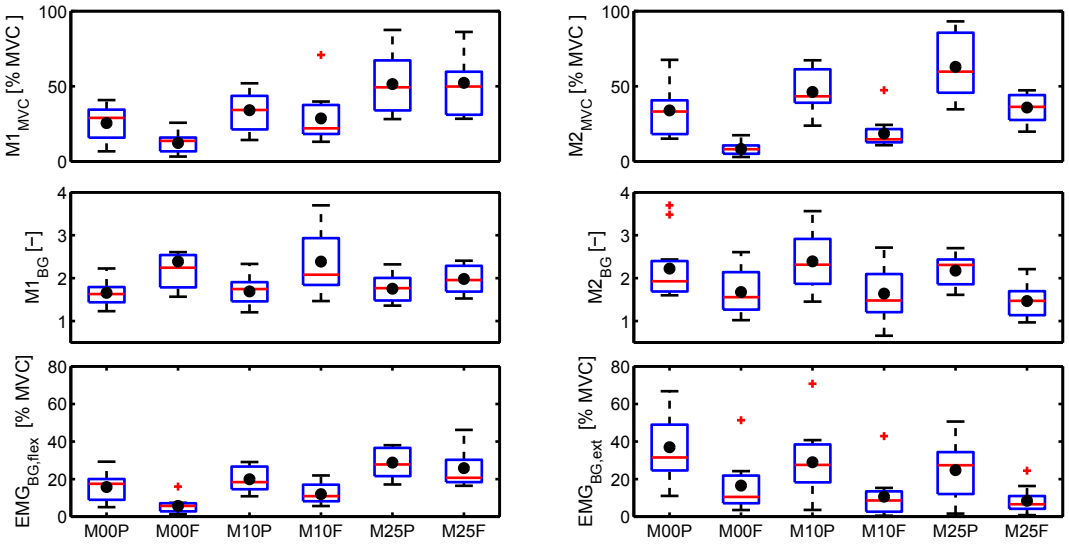

Figure C.3: PT FT conditions - 11 subjects. M1, M2 in $\%MVC$ or normalized to $EMG_{BG,flex}$ and the background activation of flexor ($EMG_{BG,flex}$) and extensor carpi radialis ($EMG_{BG,ext}$). Mean values shown as black dot.

Parameter Estimation

Table C.2: Condition independent parameters quantified from PT - WB conditions (B00P/B02P). Means (SD) over the 11 subjects.

Parameter	description	Mean	(SD)	unit
m	inertia	3.15	(0.52)	$[gm^2]$
b_c	grip damping	1.38	(0.59)	$[Nms/rad]$
k_c	grip stiffness	53.98	(43.69)	$[Nm/rad]$
F_0	activation dynamics eigenfrequency	1.6	(0.77)	$[Hz]$
T_d	neural time delay	26.6	(10.8)	$[ms]$

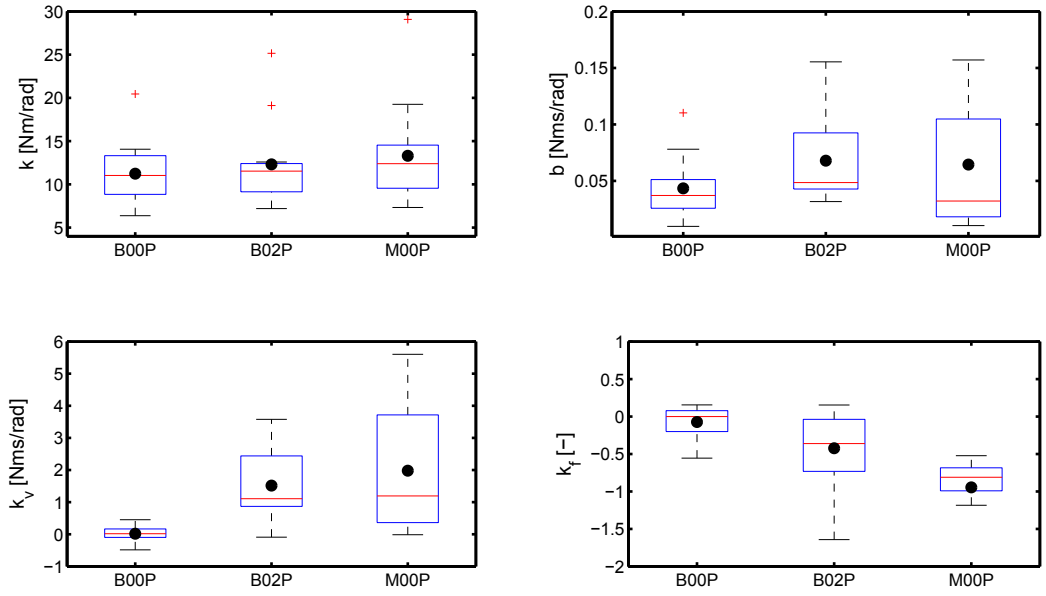

Figure C.4: PT conditions - 11 subjects.

Table C.3: VAF values in % for PT/FT conditions. **xxx** represent unstable solutions.

	M00P		M10P		M25P	
Subject	Segment 1	Segment 2	Segment 1	Segment 2	Segment 1	Segment 2
P01	75.32	70.57	63.59	68.80	37.52	20.07
P02	63.48	59.62	66.73	60.83	63.48	54.91
P03	84.43	82.63	82.56	77.77	72.12	60.89
P04	58.81	43.39	71.04	52.47	37.25	63.09
P05	72.65	85.75	77.19	79.93	73.84	82.21
P06	79.90	74.58	47.42	53.76	58.28	65.99
P07	63.96	65.28	58.48	60.91	55.55	56.94
P08	74.10	71.58	70.49	61.54	**xxx**	**xxx**
P09	**xxx**	**xxx**	80.63	69.57	69.62	70.88
P10	81.18	81.58	83.78	83.15	74.85	79.85
P11	67.37	75.40	72.06	79.53	63.30	77.92
	M00F		M10F		M25F	
Subject	Segment 1	Segment 2	Segment 1	Segment 2	Segment 1	Segment 2
P01	24.16	30.28	**xxx**	**xxx**	**xxx**	**xxx**
P02	51.90	48.22	11.94	11.27	**xxx**	28.57
P03	60.27	76.37	**xxx**	16.72	48.68	63.26
P04	**xxx**	**xxx**	**xxx**	**xxx**	**xxx**	**xxx**
P05	62.90	75.67	70.64	68.75	46.68	61.07
P06	49.75	66.46	**xxx**	**xxx**	67.40	**xxx**
P07	62.55	73.20	75.26	57.37	39.59	**xxx**
P08	75.48	80.85	**xxx**	51.05	**xxx**	32.83
P09	68.38	82.84	58.21	71.66	**xxx**	**xxx**
P10	18.22	65.58	31.44	51.68	**xxx**	40.47
P11	69.70	83.22	53.75	74.12	51.41	52.65